Journal of Microscopy, Vol. 171, Pt 2, August 1993, pp. 95–105.
Received 20 November 1992; accepted 8 March 1993

REVIEW

Near-field optical microscopy in transmission and reflection modes in combination with force microscopy

N. F. VAN HULST, M. H. P. MOERS & B. BÖLGER
Department of Applied Physics, University of Twente, PO Box 217, 7500AE Enschede, the Netherlands

Key words. Scanning probe microscopy, near-field optics, evanescent wave, SNOM, atomic force, AFM, development, feedback, correlative imaging, integrated microscopes.

Summary

Near-field optical microscopy is the optical alternative of the various types of scanning probe microscopes. The technique overcomes the classical diffraction limit in conventional optical microscopy. In this paper the concepts of near-field optics (NFO) are introduced, followed by a short review of current trends in NFO microscopy. Specifically, developments concerning the efficiency and versatility of both aperture and dielectric probe types are discussed. We present our advances in NFO microscopy, using both fibres and integrated silicon nitride (SiN) structures as dielectric probes. The use of an SiN probe as a combined optical and force sensor is shown to be advantageous, as it provides a feedback mechanism and allows direct comparison between topography and dielectric effects. Images of technical and biological samples are presented with a lateral resolution down to 20 nm, depending on the microscopical arrangement used.

Introduction: the concept of near-field optics

Far-field imaging

In conventional optical microscopy propagating waves, $\exp(ikr)$, with wave vector k propagating along a direction r, are detected in the far field, i.e. $kr \gg 1$. Many contrast mechanisms are possible, depending on whether amplitude, phase or polarization is detected. Although detection of phase gives a resolution down to the nanometre scale, the lateral resolution Δx is limited by diffraction to the size of the wavelength λ, as expressed in the common Rayleigh criterion,

$$\Delta x \geqslant 0{\cdot}61 \frac{\lambda}{n \sin \theta},$$

where n is the refractive index of the medium and θ is the acceptance angle of the detection system. As a consequence, the lateral resolution can only be improved by applying a high numerical aperature (NA $= n \sin \theta$), by decreasing the wavelength or by optimizing the modulation transfer function, as is done in confocal microscopy. Exceptional approaches along these lines have been presented by Mansfield & Kino (1990), who built a solid immersion system with $n = 2$, and by van der Oord *et al.* (1992), who demonstrated 70-nm lateral resolution in a confocal microscope with UV radiation ($\lambda = 200$ nm).

Near-field imaging

In this context a more instructive equation can be derived from Heisenberg's principle of uncertainty, $\Delta x \Delta p_x \geqslant h$, where p_x is the associated photon momentum in direction x given by $p_x = |p| \sin \theta = (hn/\lambda) \sin \theta$. Taking the allowed range of real values of p_x this leads to a similar resolution criterion,

$$\Delta x \geqslant \frac{\lambda}{2n \sin \theta}.$$

In near-field imaging the non-propagating field diffracted by a sample is detected, i.e. $kr \ll 1$. This localized form of detection with $\Delta x \ll \lambda/2$, implies the occurrence of higher spatial frequencies in the associated momentum p_x in order to fulfil the uncertainty relation. Consequently, the range of Δp_x should be larger than the absolute value $|p|$, which is only possible for imaginary values of p_x. The corresponding imaginary wave vector k reduces the propagating wave $\exp(ikr)$ to an evanescent wave $\exp(-|k|r)$ which is confined to the near-field regime.

As an example consider the radiating dipole: it radiates in the direction perpendicular to the dipole direction, while the field distribution in other directions is non-radiating and

© 1993 The Royal Microscopical Society

confined to the dipole source. A complementary example is that of an illuminated subwavelength size aperture in a conducting screen: it acts as a magnetic dipole source in the far-field direction perpendicular to the aperture, while in the near field it has both electric and magnetic dipole character with the field distribution determined by boundary conditions.

Evanescent waves can be of advantage in conventional optical microscopy for selective illumination or improvement of the vertical sensitivity, as shown by Guerra (1990) and Murray & Eshel (1992). However, lateral resolution is still diffraction limited in these systems.

The concept of near-field optical imaging beyond the diffraction limit was formulated by Synge (1928) and O'Keefe (1956) while the first experimental demonstration was given by Ash & Nicholls (1972) using microwave radiation. Experimental near-field microscopy in the optical domain has been stimulated mainly by the invention of scanning tunnelling microscopy (STM; see Pohl, 1990). Among the various forms of scanning probe microscopy, the scanning near-field optical microscope is generally referred to as SNOM.

Trends in experimental near-field optical microscopy

The progress in experimental near-field optical (NFO) microscopy over the last 10 years (see Pohl, 1990, 1993) has been mainly determined by developments in fabrication of suitable probes. Currently used NFO probes can generally be divided into aperture probes and dielectric probes.

Aperture probes

In this approach the far field penetrating through a subwavelength aperture is detected. The far-field signal is modulated by the near-field interaction of a sample in close proximity to the aperture. The aperture probe is a sharpened dielectric tip coated with metal, leaving an aperture at the apex with a 20-nm diameter as a practical lower limit. The probe can be a sharpened quartz rod (Dürig *et al.*, 1986), a pulled micro-pipette (Betzig *et al.*, 1987; Cline *et al.*, 1992) or an aperture in a metal film (Fischer *et al.*, 1988). Betzig *et al.* (1991) have obtained a major improvement in these probes by pulling adiabatically tapered single-mode fibres which enable us to illuminate the aperture with a higher efficiency. Fabrication of these probes is reproducible with a high yield if a well-controlled fibre heating and pulling system is used. The probes can be used as an NFO source or detector both in transmission and reflection. The minimum size of the aperture is determined by the finite skin depth of the metal used for the coating. Aluminium is most suitable for this purpose with 6·5-nm skin depth at $\lambda = 500$ nm. In order to provide sufficient discrimination against directly transmitted far-field contributions, a 100-nm Al coating is required. The brightness of the NFO source is determined by the residual transmissivity of the aperture and the damage threshold of the metal. The fraction of transferred light power is typically 10^{-5} for an 80-nm aperture, yielding 0·20 μW brightness with 20 mW illumination. The efficiency decreases rapidly with the sixth power of the aperture size. With these probes Betzig *et al.* (1991) have obtained 12-nm lateral resolution. Application to many optical contrast methods, such as polarization, refractive index differences and fluorescence, has been demonstrated (Betzig *et al.*, 1992c; Betzig & Trautman, 1992; Trautman *et al.*, 1992). Recently, the technique was used to read and write magneto-optical domains to a resolution of 60 nm (Betzig *et al.*, 1992b). The application of metal-coated aperture probes is limited to samples with gentle surface structure, as the outer diameter of the probe is about 0·25 μm. For routine operation a distance regulation mechanism is required.

Dielectric probes

In this approach the non-radiative near field is detected by conversion of evanescent waves into propagating waves. Usually an evanescent wave is generated at the sample surface by total internal reflection. The evanescent wave is frustrated by a sharp dielectric probe and converted into a propagating wave. This localized form of frustrated total internal reflection (FTR) has been demonstrated by several groups in recent years (Courjon *et al.*, 1989; de Fornel *et al.*, 1989; Paesler *et al.*, 1990; Reddick *et al.*, 1990; Jiang *et al.*, 1991), including our group (van Hulst *et al.*, 1991). Due to similarities with electron tunnelling, this technique is often referred to as photon scanning tunnelling microscopy (PSTM). Generally the probe is a fibre, sharpened by chemical etching or pulling. An advantage of PSTM is that it circumvents the problem of aperture fabrication and that the sharp apex allows imaging of steep structures. A lateral resolution of 10–50 nm has been claimed, based on edge steepness (Courjon *et al.*, 1989; van Hulst *et al.*, 1992a). Another advantage of PSTM is the exponential decay of the evanescent wave which provides an optical feedback mechanism to prevent the tip from crashing to the sample, analogous to the feedback in STM. The fraction of transferred light power in PSTM is of the order of 10^{-7} for a 50-nm tip apex.

However, PSTM also has an intrinsic disadvantage. With a real sample, with topographic and dielectric surface variations, both evanescent waves and propaging waves are generated by scattering, and cannot be discriminated in the waves propagating into the dielectric probe. In such cases the distance dependence of the optical coupling will no longer be exponential, making optical feedback impossible, or at least unpredictable (de Fornel *et al.*, 1992; van Hulst *et al.*, 1992b). Consequently PSTM images generally display a

combination of localized near-field and long-range far-field effects. High-resolution NFO imaging is only possible at short distances (below 20 nm), where the near field is dominant over any far-field contribution. Again a distance regulation mechanism independent of the optical properties of the sample is required.

In this paper we will present an alternative to the PSTM, taking advantage of the micro-fabricated SiN probes commonly used in atomic force microscopy (AFM). These probes can be operated in close contact, acting simultaneously as an optical and a force probe (van Hulst *et al.*, 1992c).

Passing the efficiency barrier

The efficiency of an NFO probe is limited by two aspects. First, the transition from the far field to the cut-off dimensions of the probe has to be overcome with minimal loss of light power. The adiabatically tapered fibres developed by Betzig *et al.* (1991) are optimized in this respect. A second, more fundamental, limit is the transition to the actual subwavelength dimensions of the probe, as there are no propagating modes to support the energy transport in this regime. For an aperture probe the efficiency varies with the fourth power of the aperture size (Dürig *et al.*, 1986). Fischer & Zepletal (1992) have addressed this problem by fabricating an optical coaxial line, i.e. an optical fibre with a metal core, which allows a propagating mode without cut-off. This approach seems promising, but realizing it is a technological challenge. A different approach by Lewis & Lieberman (1991) is based on the use of excitons for energy transport. They filled metal-coated pipettes with fluorescent dye, thus generating a true radiating fluorescence light source about 50 nm in dimension with relatively high brightness. Although application of these probes is restricted to flat samples, images with about 0·2-μm lateral resolution have been obtained. Excitation of a plasmon resonance can also enhance the sensitivity. Specht *et al.* (1992) have advantageously implemented the excitation of a surface plasmon in an STM configuration and obtained 3-nm optical lateral resolution on an silver surface. Excitation of a localized plasmon has been observed by Fischer & Pohl (1989).

Combinations with force microscopy

As pointed out, a reliable feedback mechanism, which controls the distance between probe and sample independent of optical properties, is essential in NFO imaging. Dürig *et al.* (1986) successfully applied electron tunnelling feedback on a conductive sample; however, for general application to dielectric surfaces force feedback is more suitable. Recently, several groups have reported on force regulation in NFO microscopy. Toledo-Crow *et al.* (1992) and Betzig *et al.* (1992a) have introduced a small lateral oscillation at about resonance at their aperture probe. By detection of the so-called 'shear force' in a dynamic scheme, they showed both force feedback and simultaneous NFO and force imaging. Clearly shear force feedback will also be of advantage in PSTM. A system based on vertical force feedback, using a micro-fabricated Si membrane with an aperture, was demonstrated by Prater *et al.* (1991), but optical resolution was still limited to 0·25 μm. Preliminary results with an SiN NFO probe, allowing both vertical and lateral force detection, have been reported by van Hulst *et al.* (1992c). Recently, Shalom *et al.* (1992) proposed the use of bent micro-pipettes for vertical force detection. In this context, a paper by Malmqvist & Hertz (1992) should also be mentioned, where a subwavelength size particle, optically trapped by radiation pressure, was used for NFO imaging.

Other approaches with dielectric probes

We have developed different types of microscopical arrangements, each with their specific advantages and disadvantages. A schematic overview of the different configurations is displayed in Fig. 1. We have used etched fibres and SiN probes both in transmission and reflection configurations. Experimental details, results and specific aspects of each configuration will be discussed in the following sections.

Fibre probes

Transmission. This configuration, as sketched in Fig. 1(a) is the normal photon scanning tunnelling microscope (PSTM) set-up. An evanescent field generated by total internal

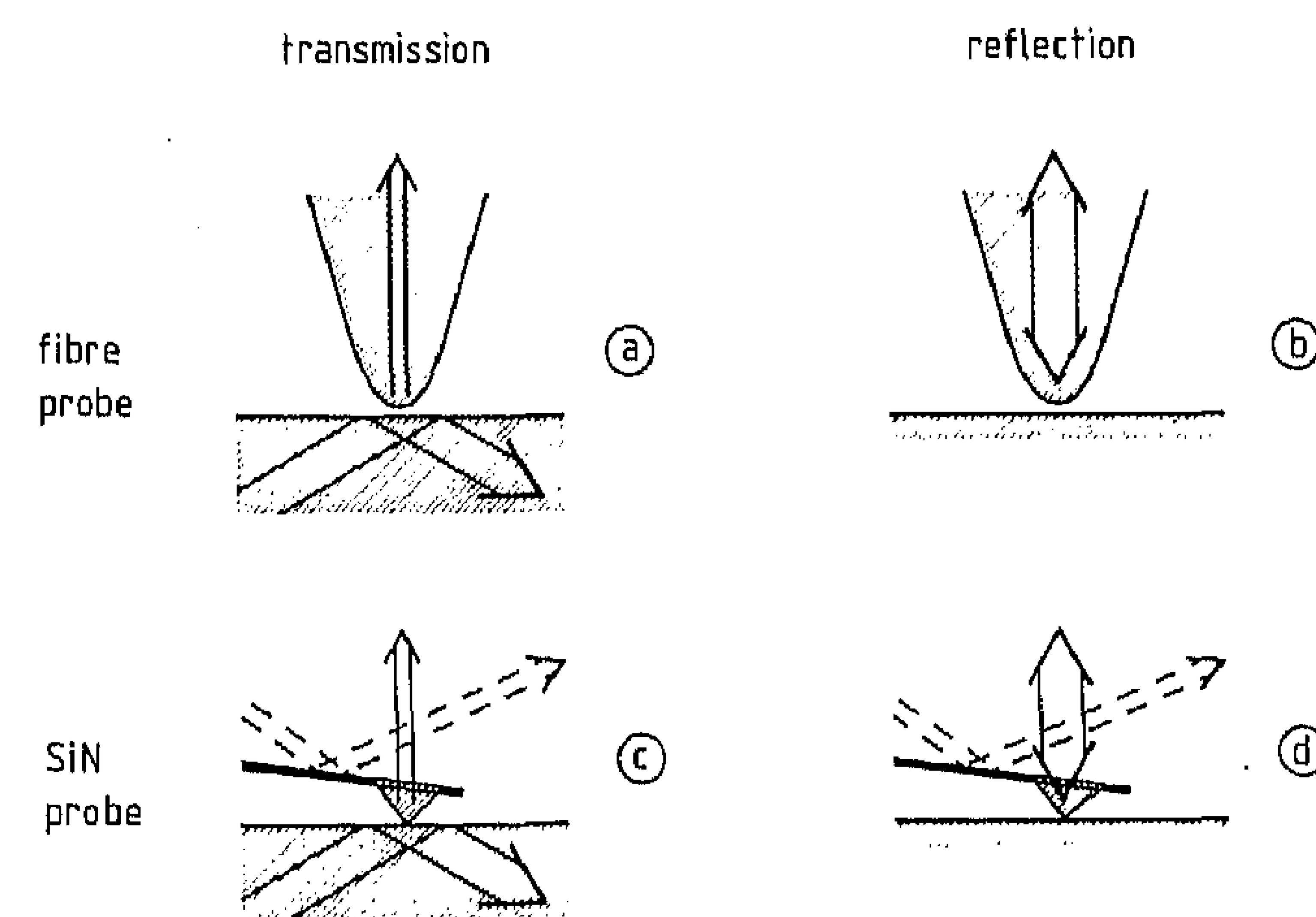

Fig. 1. Schematic overview of the near-field optical (NFO) microscope configurations built in our laboratory based on either fibre probes or micro-fabricated SiN probes with light incident by total internal reflection (transmission) or into the probe (reflection). Solid arrows: light path for NFO detection. Dashed arrows: optical beam deflection path for force detection.

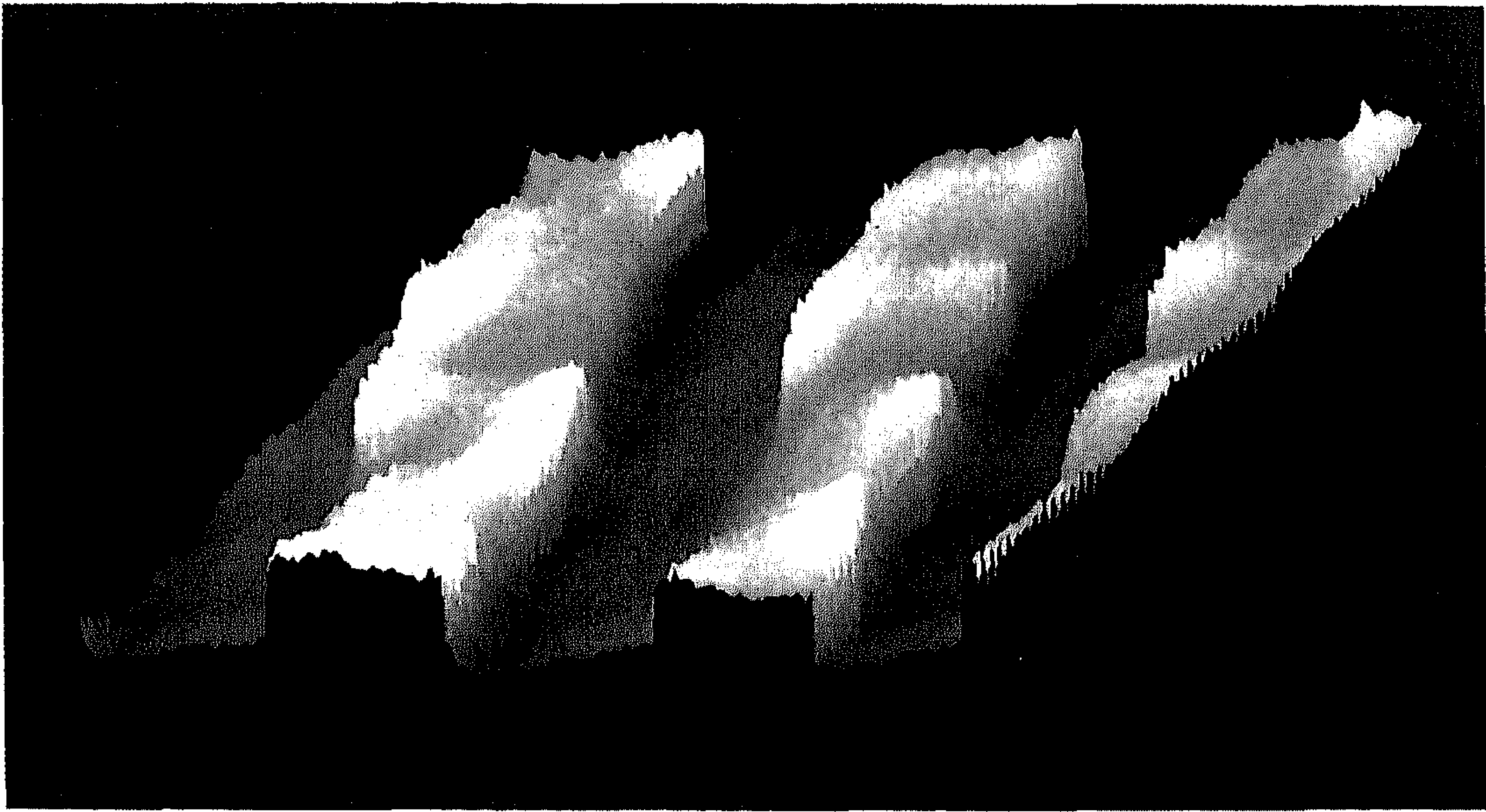

Fig. 2. Photon scanning tunnelling microscopy image of an SiN grating with trenches 500 nm wide and 350 nm high. Scanned in optical feedback over $2{\cdot}6 \times 2{\cdot}6\ \mu m$.

reflection is locally frustrated by a sharpened fibre. We have imaged gratings and spheres which were prepared on a microscope cover slip which is placed on the substrate with an index-matching liquid.

Figure 2 shows a three-dimensional (3-D) display of a PSTM image, scanned in optical feedback, of a 1-μm-period SiN grating. The grating has been fabricated by lithographic etching of a PECVD (plasma enhanced chemical vapour deposition) SiN layer. The fibre tip follows the grating contour of 500-nm width and 350-nm height with an edge steepness of about 30 nm, resulting in a mainly topographic image. Considering the wavelength of the light source (632·8 nm), the edge steepness is far beyond the diffraction limit.

Figure 3 shows the detected field distribution close to a 91-nm latex sphere, obtained by scanning at constant height. The image has been differentiated in order to enhance the fringe-like patterns surrounding the sphere. The pattern is caused by interference between the evanescent wave, propagating parallel to the surface, and the near-field distribution caused by scattering at the sphere (van Hulst *et al.*, 1992b). Thus the pattern contains both amplitude and phase information on the near-field Fresnel diffraction by the sphere. This field distribution cannot be detected by any far-field technique.

Although PSTM is capable of superresolution, the technique is limited to transparent objects and samples which exhibit only a limited scattering contribution, i.e. low-relief surfaces.

Reflection. In this arrangement (Fig. 1b) the probe is again formed by a sharpened fibre. An evanescent field is generated at the end of the fibre itself by coupling light into the fibre and reflecting it at the sharpened end where the dimensions are below the cut-off size. A dielectric sample brought in close proximity frustrates the evanescent wave which affects the detected intensity of the reflected light. The presence of a sample changes the reflected signal by less than 1% for transparent surfaces and by up to 10%

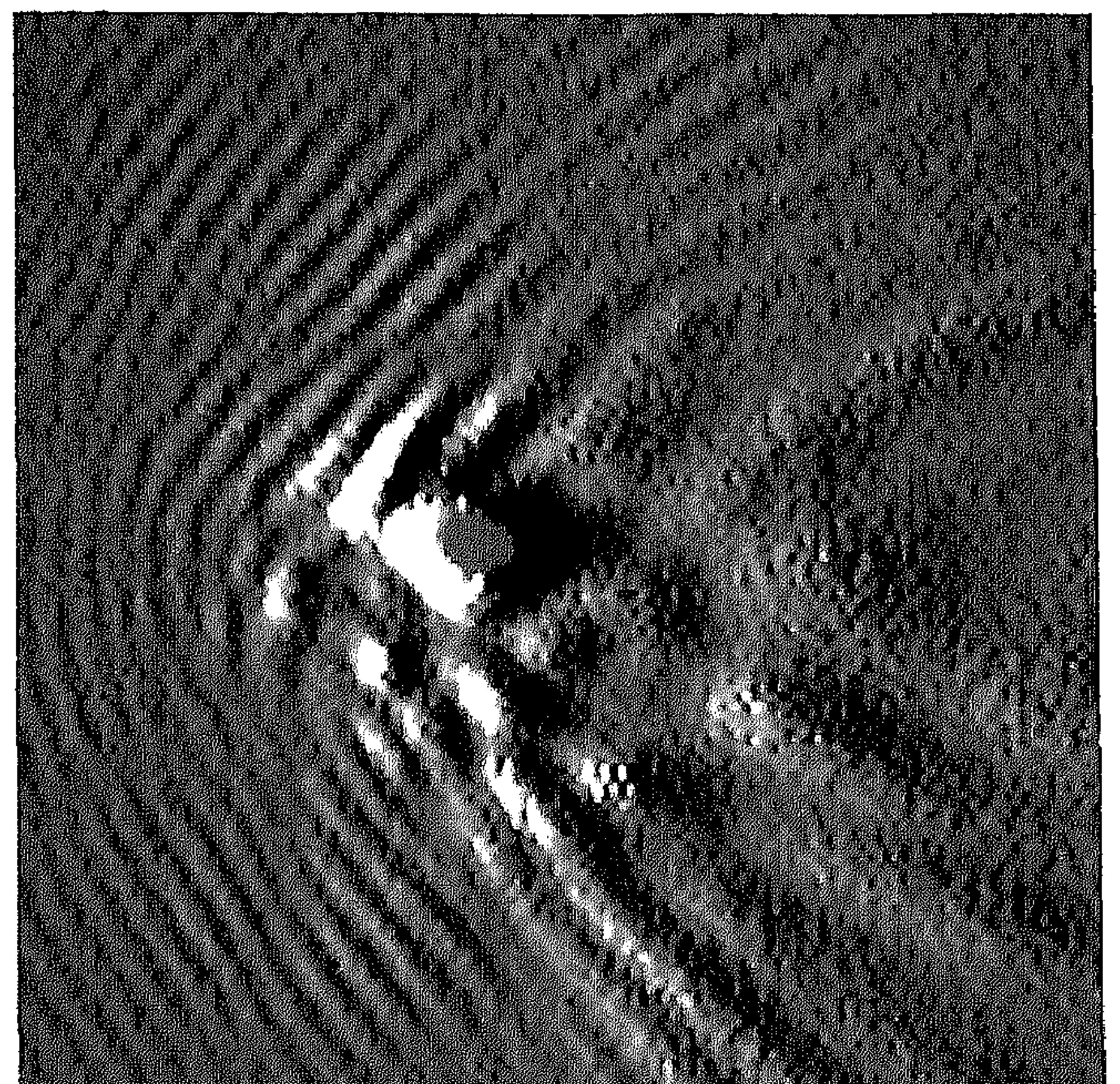

Fig. 3. Constant-height photon scanning tunnelling microscopy image ($9 \times 9\ \mu m$) of a 91-nm latex sphere. The laser beam incident at total internal reflection propagates from left to right.

for highly reflecting surfaces. An image is obtained by scanning the sample at constant distance to the tip, without feedback. A similar 'external reflection' microscope has been reported by Courjon & Spajer (1991).

As the fibre approaches the sample surface, a Fabry Perot fringe pattern is observed with increasing amplitude towards the surface, until an abrupt signal change is observed, corresponding to the near-field regime. The near-field behaviour depends largely on the sample surface and the fibre tip.

As a test structure we have chosen a polycarbonate compact disc (CD), consisting of indented tracks with 1·25 μm period and pits 200 nm in diameter. The sample has been coated with silver for higher reflectivity. Figure 4 shows a 9×9-μm 3-D image of the reflection signal over the CD, displaying both circular pits and long trenches, scanned at a constant height of about 100 nm. The indented pits appear to enhance the reflected signal relative to the surrounding area. Their apparent diameter is about 500 nm, while the actual diameter is 200 nm. The signal level directly beside the pits is slightly below the average signal level of the surrounding area. The trenches appear as a decrease in the average reflectivity, whereas the intermediate region appears more pronounced with a stronger signal decrease. The appearance of the trenches is probably dominated by mutual interference of the reflected light from adjacent trenches. Courjon & Spajer (1991) have also observed an enhanced reflection signal in grating grooves and similar oscillatory patterns superimposed over the actual structure. A theoretical analysis by Girard & Spajer (1990) shows that fringe-like patterns can indeed be expected in reflection imaging.

As another example we have imaged a K562 cell. The K562 cells from a human cell line are adhered to and air dried on a poly-L-lysine-coated microscope slide. The cell can be clearly recognized in the reflection image (Fig. 5), with enhanced reflectivity at the edges and centre, separated by a darker intermediate area. The appearance is probably an optical effect, as the topography studied by AFM (Putman *et al.*, 1992) generally displays a more constant cell height. The image illustrates that imaging of biological objects is possible; however, for interpretation the optical contrast mechanism should be carefully analysed.

The lateral resolution in this reflection configuration is about 100 nm, mainly determined by the sharpness of the tip, the finite working distance and the effective numerical aperture (NA) of the tip for reflected light. We have observed the effects of polarization and tip shape. For quantitative imaging a reliable feedback mechanism is indispensable.

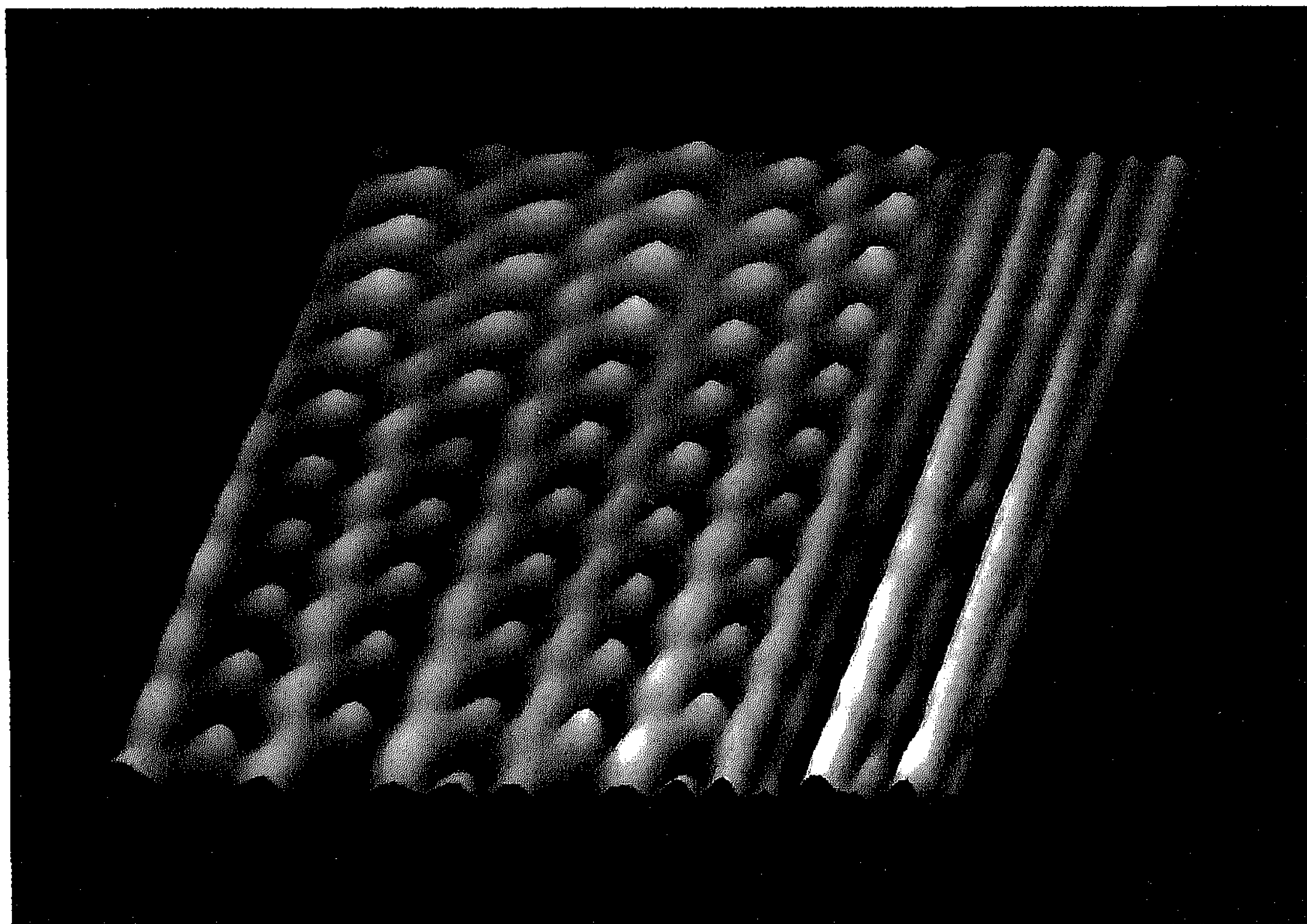

Fig. 4. Reflection near-field optical image of a compact disc structure with silver-coated circular pits (200 nm) and trenches with 1·25-μm period. Scanned at constant height over 9×9 μm.

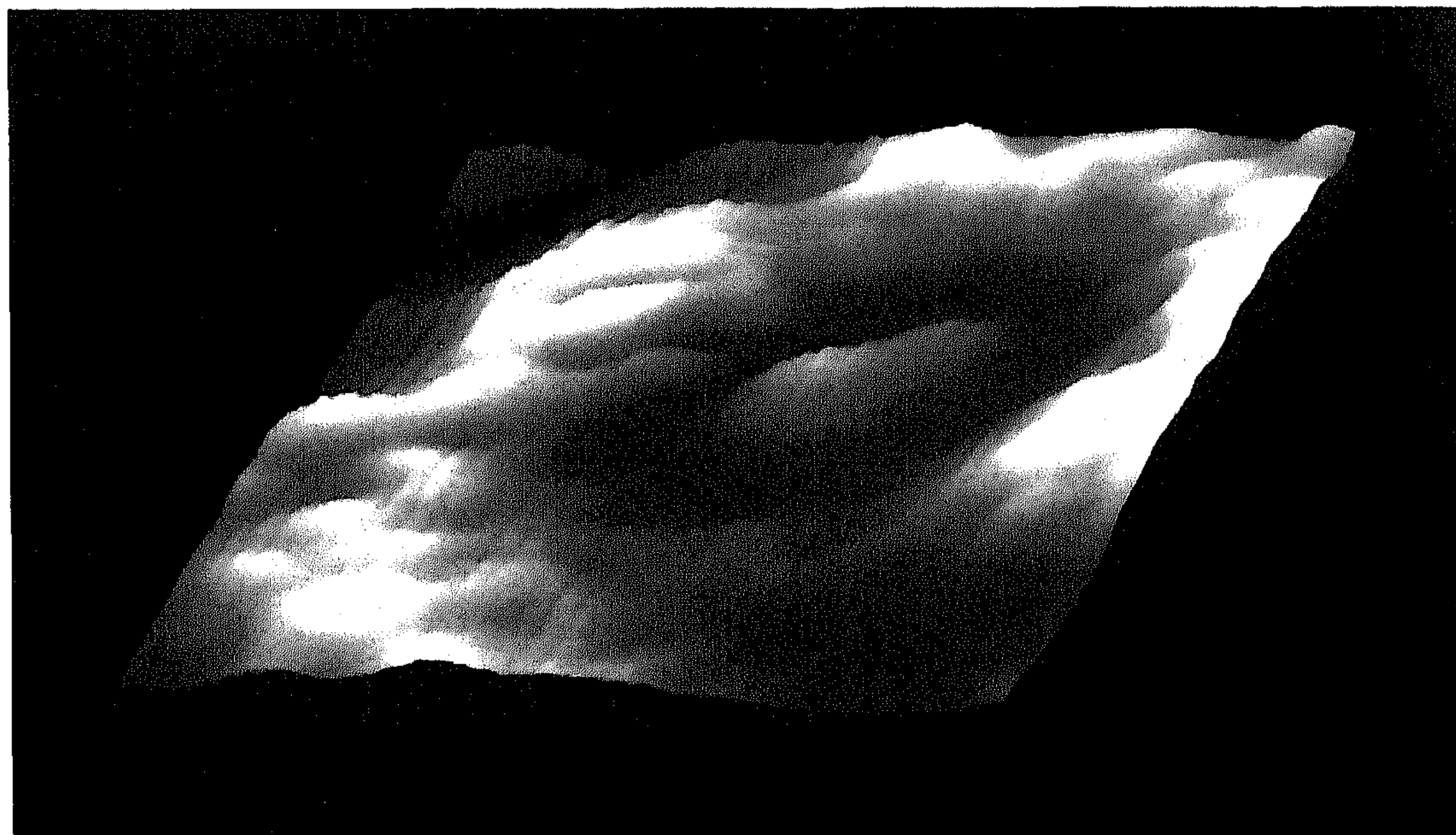

Fig. 5. Reflection near-field optical image (10 × 10 μm) of a K562 cell.

Micro-fabricated probes: combined force and optical microscopy

The main limitation of microscopes based on optical fibres is that in close distance operation without feedback a single touch to the sample surface is generally disastrous. Yet a distance below 20 nm is essential for high-resolution NFO imaging. On arbitrary surfaces this can only be accomplished by installing a reliable feedback mechanism, independent of the optical properties of the sample. We present an alternative approach in which we take advantage of the unique features of the micro-fabricated SiN probes (Park Scientific Instruments) commonly used in AFM. These probes consist of a pyramidal SiN tip with 20–50-nm apex and are integrated on a cantilever with low spring constant (0·06 N/m) such that they can be scanned with a low interaction force in close contact over a surface. The interaction force is determined by measuring the bending of the cantilever. SiN has ideal mechanical strength and properties for micro-fabrication, and it is also a good optical material ($n = 2{\cdot}0$) with transparency down to 290 nm. Thus the SiN probe is a high-index optical structure with 20–50-nm apex, i.e. an ideal NFO probe, with the advantage that it simultaneously acts as a force probe.

Transmission. The experimental arrangement is sketched in Fig. 1(c). As with the PSTM set-up, an evanescent wave is generated on a glass substrate by total internal reflection of a laser beam. However, in this set-up the optical probe is formed by an SiN cantilever with integrated pyramidal tip. A long-working-distance objective collects the light generated by FTR (frustrated total internal reflection) at the SiN apex. A pinhole in the imaging plane is adjusted such that only light from the SiN apex passes onto the detector. A second optical path is formed by a laser diode focused onto the cantilever where the reflected beam is detected on a split detector. This optical beam deflection system (Meyer & Amer, 1988) enables detection of both cantilever deflection and torsion caused by the interaction force between tip and sample. A near-field optical and a force image are obtained simultaneously by scanning the sample in contact with the probe, either in open loop or at constant force with a feedback on the beam deflection signal. As the probe approaches the sample surface an exponential increase in the optical signal is observed, corresponding to the coupling to the exponentially decaying evanescent wave. At some distance the tip jumps into contact caused by the water film on the surface. The adhesion force is of the order of 10 nN, which is a typical value for an air-operated force microscope (Weisenhorn *et al.*, 1989).

Figure 6 displays AFM and NFO images of the same 1-μm-period SiN grating displayed in Fig. 2. In the force image the 500-nm glass trenches between the SiN lines are reduced to 175 nm due to a tip convolution effect. In the optical image the lower glass trenches appear light against the SiN top layer because of the different optical coupling efficiencies for glass and SiN to the SiN probe. The observed contrast can also be influenced by partial reflection at the glass–SiN transition within the sample.

Figure 7 shows corresponding AFM and NFO scans over an indium–tin-oxide film (Baltracon). In order to avoid tip

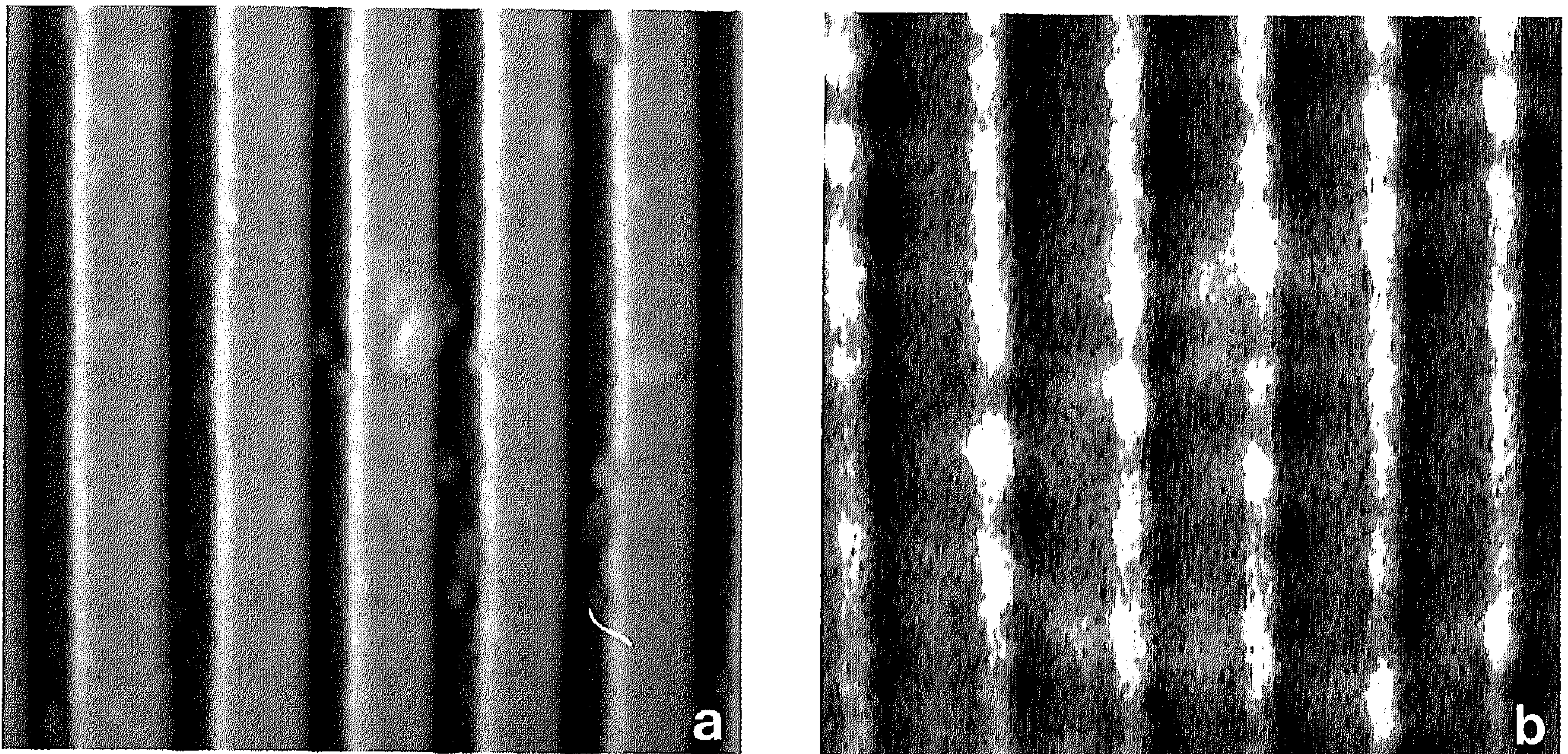

Fig. 6. A 5·5 × 5·5-μm scan of a 1-μm-period SiN grating: (a) atomic force microscope image in height mode; (b) optical image with SiN probe in transmission.

convolution effects on this rough sample, an SiN tip with a small electron beam deposited needle was used (a so-called 'supertip'; Keller & Chih-Chung, 1992). Crystallites about 50 nm in size are clearly resolved in the force image. In the optical image similar structures are resolved, but the grains appear dark against the background due to their higher refractive index and limited transmissivity. Between the grains rather sharp light rims are observed with a width of about 20 nm.

The light path after the objective is partly split towards a camera which facilitates alignment of the system and location of a sample area. This feature is particularly important for locating isolated biological objects. As an example, metaphase Chinese hamster lung chromosomes,

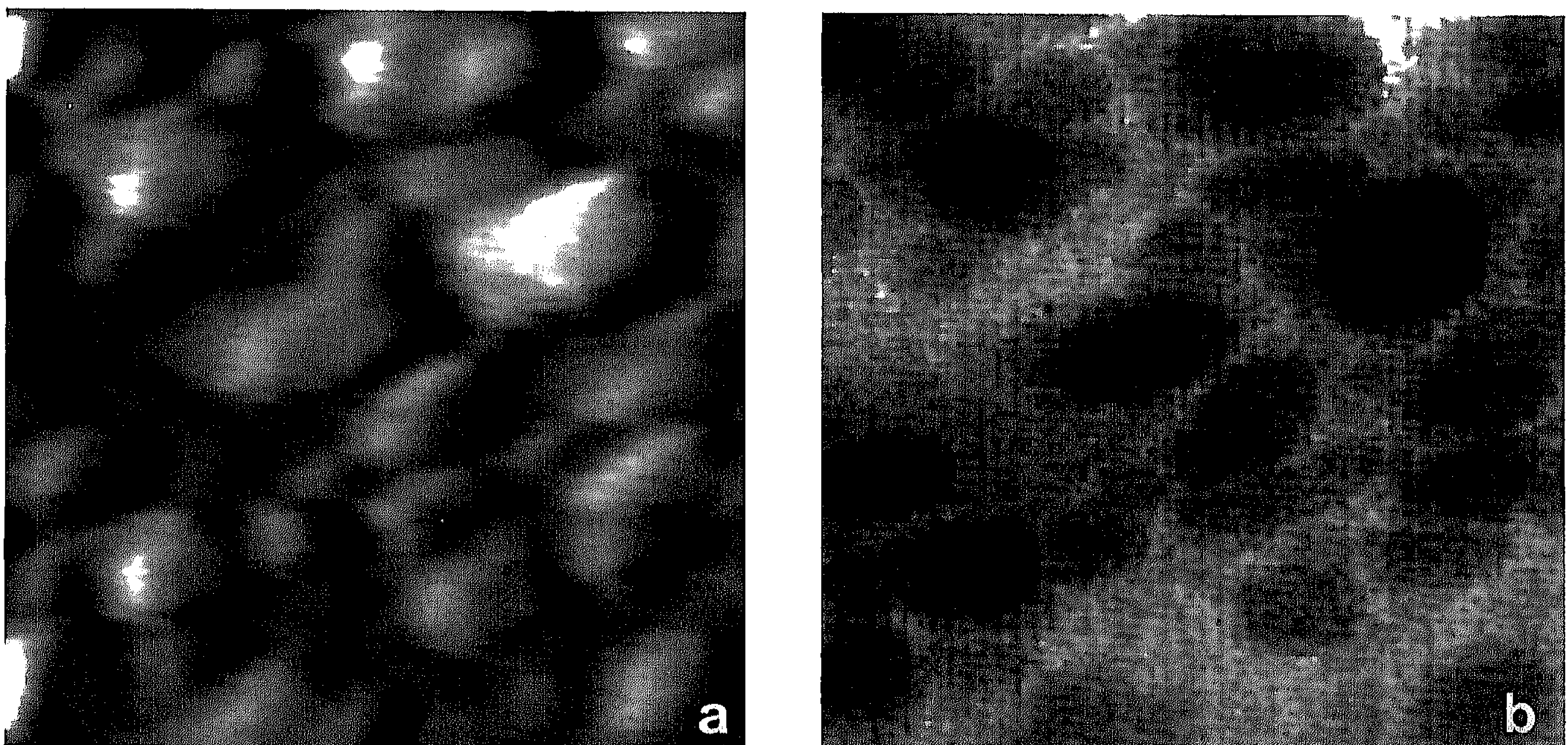

Fig. 7. Indium–tin-oxide grains (scan area of 500 × 500 nm): (a) atomic force microscope image; (b) corresponding optical image scanned with a 'supertip'.

which were recently investigated by force microscopy (de Grooth & Putman 1992), were examined. The corresponding AFM and NFO images are shown in Fig. 8. The AFM image displays the topography. In the NFO image the chromatides appear to reduce the optical coupling, causing parts of the chromosome to appear dark. Simultaneously, the scattering at the chromosome causes a rather intense radiative contribution to the right of the chromosome and interference fringes at the other side of the chromosome.

This experimental configuration allows routine scanning with a high optical lateral resolution, but interference effects can be dominant on surfaces which display extensive scattering.

Reflection. This set-up is shown in Fig. 1(d). Again, the heart of the instrument is a commercial micro-fabricated SiN probe. A laser beam is focused at normal incidence into the rear of an SiN tip using a high-NA objective. The laser spot at the cantilever, 2–3 μm in diameter, fits within the area of the pyramidal tip. At the apex of the illuminated tip an evanescent wave is created, while part of the light is transmitted as a radiative wave. The tip apex is confocally imaged onto a pinhole which is chosen such that only the beam reflected at the centre of the tip is passed onto a detector. In addition, this set-up is equipped with an optical beam deflection system for force detection. Beneath the sample we have constructed an inverted optical microscope with epi-illumination, following the design of Putman *et al.* (1992), which facilitates simultaneous viewing of the sample, the position of the tip over surface, the position of the laser beam in the SiN pyramid and the position of the beam deflection spot on the cantilever.

Figure 9 shows images obtained with the combined NFO–AFM reflection system on a CD test structure, similar to that in Fig. 4, this time with trenches spaced at 1·25 μm and pits 1·0 μm in length. Figure 9 displays the simultaneously recorded AFM and NFO images. The force image corresponds to the topographic structure, in which the finest detail of about 30 nm is determined by the tip sharpness, while the optical image corresponds to changes in the effective reflectivity. The NFO image is similar both in force feedback and in open loop, indicating that the effect of bending of the cantilever on the optical image is limited.

Figure 10 displays the corresponding AFM and NFO images of a K562 cell, similar to the one in Fig. 5. The AFM image shows the cell morphology and its surroundings, where some filopodia can be vaguely recognized. The NFO image displays features distinctly different from the topography. At most positions with cell material the reflected optical signal is reduced, but at other positions it is enhanced or not correlated with topography.

The contrast in the NFO image is determined by several contributions. First, it should be realized that the reflected signal from an area 2–3 μm^2 is detected because of the diffraction limit. Consequently, in the absence of the SiN probe the system images as a confocal microscope with a lateral resolution limited by the NA of the objective. The SiN probe introduces a highly localized optical contribution and

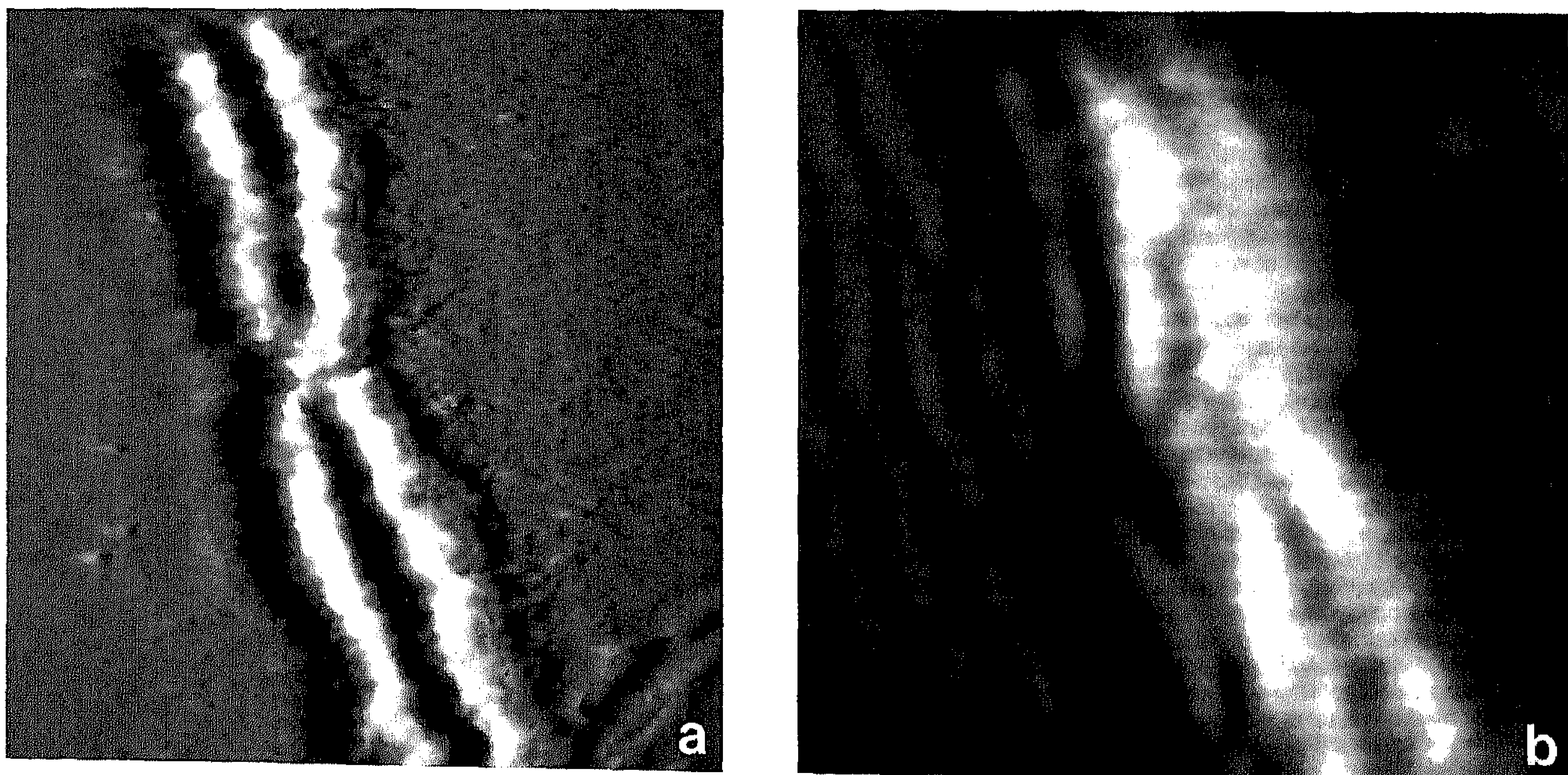

Fig. 8. Metaphase Chinese hamster lung chromosome (scan area of 10 × 10 μm): (a) atomic force microscope image; (b) corresponding optical image in transmission.

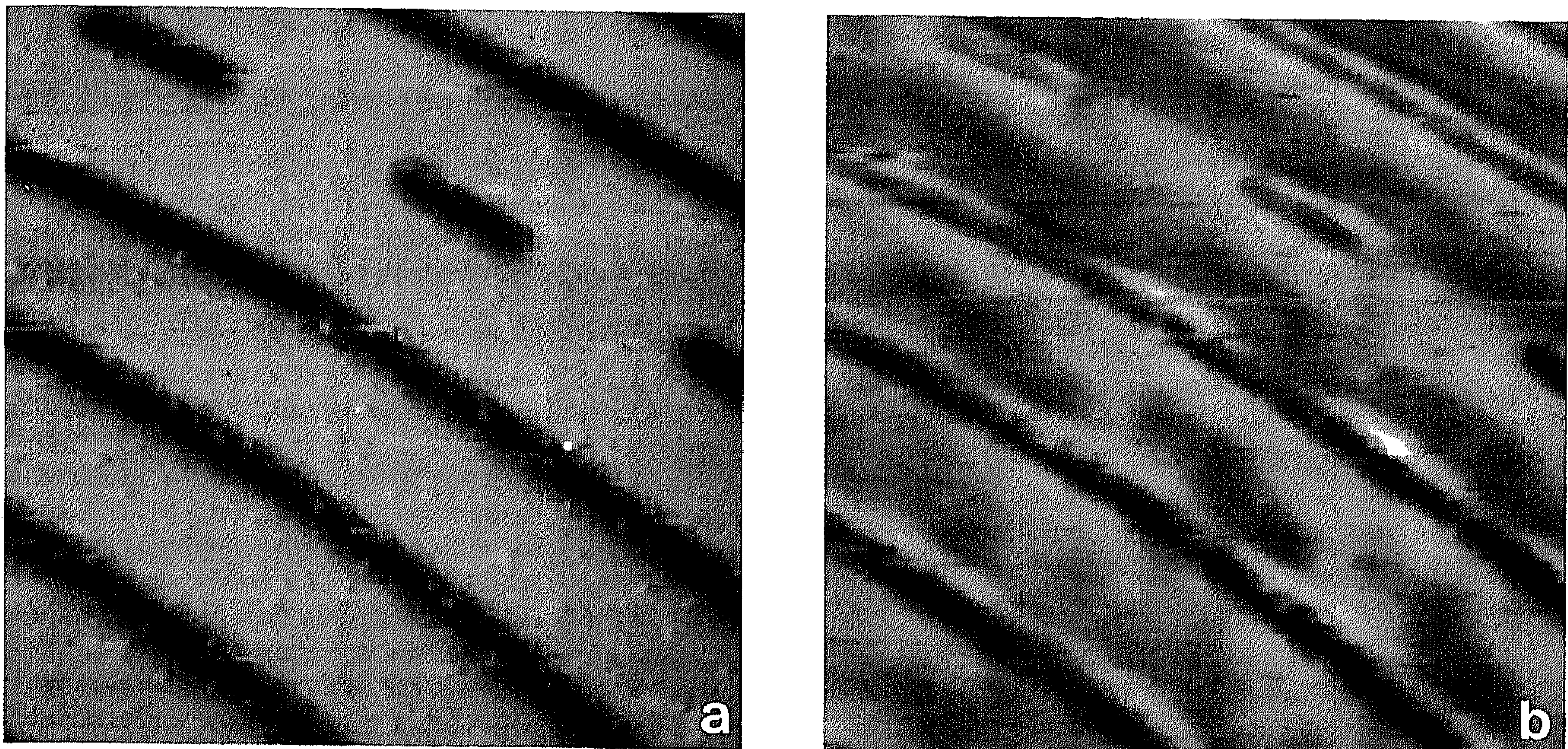

Fig. 9. A 6 × 6-μm scan of a compact disc structure with 1·25-μm-period tracks: (a) atomic force microscope image; (b) corresponding optical image in reflection.

partly obstructs the confocal image. Simultaneously, the SiN apex follows the localized variations in the surface topography which affects the reflected optical signal in the contact area. Interference between cantilever and sample surface or objective might play a role. In conclusion, the reflection NFO images contain optical contrast but high-resolution features are probably correlated with topography.

Conclusion and outlook

Several NFO microscopes based on dielectric probes have been presented, each with its specific aspects. The use of SiN probes eliminates the fundamental practical problems in earlier designs and allows routine non-destructive detection of localized FTR in close contact scanning on arbitrary surfaces. Combination with force detection provides an

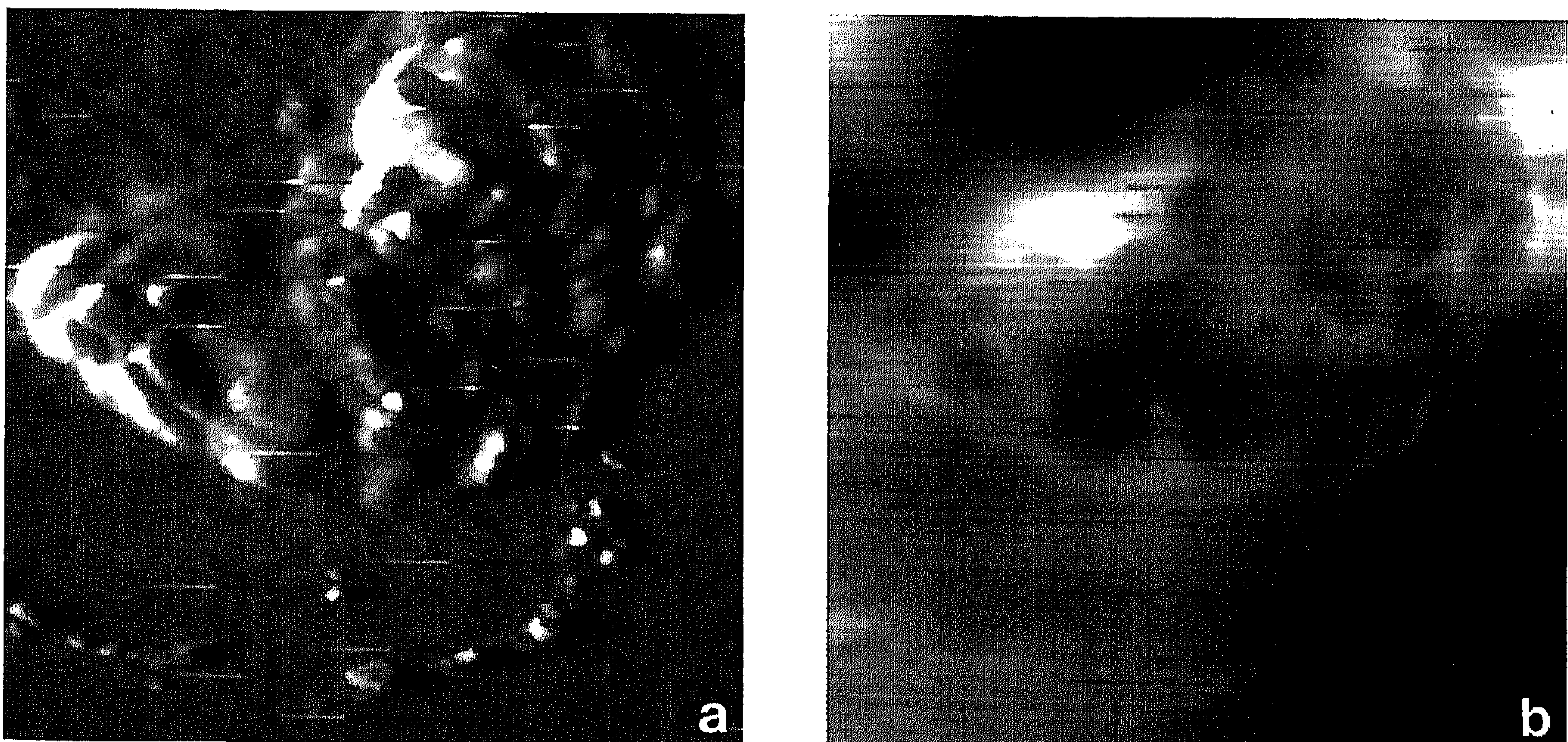

Fig. 10. Part of a K562 cell (scan area of 4 × 4 μm): (a) atomic force microscope image; (b) corresponding optical image in reflection.

independent feedback mechanism and enables discrimination between topography and dielectric properties. Integration of a conventional optical microscope proves very practical for the alignment and selection of a specific scan area. NFO images with a lateral resolution down to 20 nm have been obtained, in which the optical contrast is determined by surface topography, refractive index and transmissivity variations. Full understanding of the contrast mechanism in the various microscopical arrangements requires further theoretical modelling. The sensitivity for far-field scattering is a serious problem which limits the application of NFO microscopes based on dielectric probes.

The true advantage of near-field optics compared to other forms of scanning probe microscopy will become apparent when combined with established optical techniques, such as polarization contrast and spectroscopic analysis (e.g. fluorescent labelling). In principle, all contrast mechanisms of conventional optical microscopy can be adapted to near-field detection, resulting in a truly optical imaging device with a resolution comparable to that of an electron microscope, operating at ambient conditions or even in liquid. Application to biological (*in vivo*) and chemical samples is particularly promising.

Acknowledgments

The authors thank R. G. Tack, O. F. J. Noordman, F. J. Achten and T. Faulkner for setting up the various NFO microscopes and F. B. Segerink for technical assistance and software development. The numerous constructive suggestions of K. O. van der Werf, C. A. J. Putman and B. G. de Grooth are greatly appreciated. This research is mainly supported by the Dutch Foundation for Fundamental Research (FOM).

References

Ash, E.A. & Nicholls, G. (1972) Super-resolution aperture microscope. *Nature*, **237**, 510–512.

Betzig, E., Isaacson, M. & Lewis, A. (1987) Collection mode near-field optical microscopy. *Appl. Phys. Lett.* **51**, 2088–2090.

Betzig, E., Finn, P.L. & Weiner, J.S. (1992a) Combined shear force and near-field scanning optical microscopy. *Appl. Phys. Lett.* **60**, 2484–2486.

Betzig, E. & Trautman, J.K. (1992) Near-field optics: microscopy, spectroscopy, and surface modification beyond the diffraction limit. *Science*, **257**, 189–195.

Betzig, E., Trautman, J.K., Harris, T.D., Weiner, J.S. & Kostelak, R.L. (1991) Breaking the diffraction barrier: optical microscopy on a nanometric scale. *Science*, **251**, 1468–1470.

Betzig, E., Trautman, J.K., Weiner, J.S., Harris, T.D. & Wolfe, R. (1992c) Polarization contrast in near-field scanning optical microscopy. *Appl. Opt.* **31**, 4563–4568.

Betzig, E., Trautman, J.K., Wolfe, R., Gyorgy, E.M., Finn, P.L., Kryder, M.H. & Chang, C.-H. (1992b) Near-field magneto-optics and high density data storage. *Appl. Phys. Lett.* **61**, 142–144.

Cline, J.A., Barshatzky, H. & Isaacson, M. (1992) Scanned-tip reflection-mode near-field scanning optical microscopy. *Ultramicroscopy*, **38**, 299–304.

Courjon, D., Sarayeddine, K. & Spajer, M. (1989) Scanning tunneling optical microscopy. *Opt. Commun.* **71**, 23–28.

Courjon, D. & Spajer, M. (1991) Reflection near-field optical microscopy. *J. Phys. III*, **1**, 1–12.

Dürig, U., Pohl, D.W. & Rohner, F. (1986) Near-field optical-scanning microscopy. *J. Appl. Phys.* **59**, 3318–3327.

Fischer, U.Ch., Dürig, U.T. & Pohl, D.W. (1988) Near-field optical scanning microscopy in reflection. *Appl. Phys. Lett.* **52**, 249–251.

Fischer, U.Ch. & Pohl, D.W. (1989) Observation of single particle plasmons by near field optical microscopy. *Phys. Rev. Lett.* **62**, 458–461.

Fischer, U.Ch. & Zepletal, M. (1992) The concept of a coaxial tip as a probe for scanning near field optical microscopy and steps towards a realisation. *Ultramicroscopy*, **42-44**, 393–398.

de Fornel, F., Goudonnet, J.P., Salomon, L. & Lesniewska, E. (1989) An evanescent field optical microscope. *Optical Storage and Scanning Technology* (ed. by T. Wilson), *Proc. SPIE*, **1139**, 77-84.

de Fornel, F., Salomon, L., Adam, P., Bourillot, E. & Goudonnet, J.P. (1992) Resolution of the photon scanning tunneling microscope: influence of physical parameters. *Ultramicroscopy*, **42-44**, 422–429.

Girard, C. & Spajer, M. (1990) Model for reflection near field microscopy, *Appl. Opt.* **29**, 3726–3733.

de Grooth, B.G. & Putman, C.A.J. (1992) High-resolution imaging of chromosome-related structures by atomic force microscopy. *J. Microsc.* **168**, 239–247.

Guerra, J.M. (1990) Photon tunneling microscopy. *Appl. Opt.* **29**, 3741–3752.

van Hulst, N.F., de Boer, N.P. & Bölger, B. (1991) An evanescent field optical microscope. *J. Microsc.* **163**, 117–130.

van Hulst, N.F., Moers, M.H.P., Noordman, O.F.J., Faulkner, T., Segerink, F.B., van der Werf, K.O., de Grooth, B.G. & Bölger, B. (1992c) Operation of a scanning near field optical microscope in reflection in combination with a scanning force microscope. *Scanning Probe Microscopies* (ed. by S. Manne), *Proc. SPIE*, **1639**, 36–42.

van Hulst, N.F., Segerink, F.B. & Bölger, B. (1992a) High resolution imaging of dielectric surfaces with an evanescent field optical microscope. *Opt. Commun.* **87**, 212–218.

van Hulst, N.F., Segerink, F.B., Achten, F. & Bölger, B. (1992b) Evanescent field optical microscopy: effects of polarization, tip shape and radiative waves. *Ultramicroscopy*, **42-44**, 416–421.

Jiang, S., Tomita, N., Ohsawa, H. & Ohtsu, M. (1991) A photon scanning tunneling microscope using an AlGaAs laser. *Jap. J. Appl. Phys.* **30**, 2107–2111.

Keller, D.J. & Chih-Chung, C. (1992) Imaging steep, high structures by scanning force microscopy with electron beam deposited tips. *Surf. Sci.* **268**, 333–339.

Lewis, A. & Lieberman, K. (1991) Near field optical imaging with a non-evanescently excited high-brightness light source of sub-wavelength dimensions. *Nature*, **354**, 214–216.

Malmqvist, L. & Hertz, H.M. (1992) Trapped particle optical microscopy. *Opt. Commun.* **94**, 19–24.

Mansfield, S.M. & Kino, G.S. (1990) Solid immersion microscope. *Appl. Phys. Lett.* **57**, 2615–2616.

Meyer, G. & Amer, N.M. (1988) Novel approach to atomic force microscopy. *Appl. Phys. Lett.* **53**, 1045–1047.

Murray, J.M. & Eshel, D. (1992) Evanescent-wave microscopy: a simple optical configuration. *J. Microsc.* **167**, 49–62.

O'Keefe, J.A. (1956) Resolving power of visible light. *J. Opt. Soc. Am.* **46**, 359.

van der Oord, C.J.R., Gerritsen, H.C., Levine, Y.K., Myring, W.J., Jones, G.R. & Munro, I.H. (1992) Synchrotron radiation as a light source in confocal microscopy. *Rev. Sci. Instrum.* **63**, 632–633.

Paesler, M.A., Moyer, P.J., Jahncke, C.J., Johnson, C.E., Reddick, R.C., Warmack, R.J. & Ferrell, T.L. (1990) Analytical photon scanning tunneling microscopy. *Phys. Rev.* **B42**, 6750–6753.

Pohl, D.W. (1990) Scanning near-field optical microscopy (SNOM). *Advances in Optical and Electron Microscopy* (ed. by C.J.R. Sheppard and T. Mulvey), Vol. 12, pp. 243–312. Academic Press, London.

Pohl, D.W. (ed.) (1993) *Proc. Int. Workshop on Near Field Optical and Related Techniques.* Kluwer Academic Publishers, the Netherlands (in press).

Prater, C.B., Hansma, P.K., Tortonese, M. & Quate, C.F. (1991) Improved scanning ion-conductance microscope using microfabricated probes. *Rev. Sci. Instrum.* **62**, 2634–2638.

Putman, C.A.J., van der Werf, K.O., de Grooth, B.G., van Hulst, N.F., Segerink, F.B. & Greve, J. (1992) Atomic force microscope featuring an integrated optical microscope. *Ultramicroscopy*, **42-44**, 1549–1552.

Reddick, R.C., Warmack, R.J., Chilcott, D.W., Sharp, S.L. & Ferrell, T.L. (1990) Photon scanning tunneling microscopy. *Rev. Sci. Instrum.* **61**, 3669–3677.

Shalom, S., Lieberman, K., Lewis, A. & Cohen, S. (1992) A micropipette force probe suitable for near-field scanning optical microscopy. *Rev. Sci. Instrum.* **63**, 4061–4065.

Specht, M., Pedarnig, J.D., Heckl, W.M. & Hänsch, T.W. (1992) Scanning plasmon near-field microscope. *Phys. Rev. Lett.* **68**, 476–479.

Synge, E. (1928) Suggested method for extending microscopic resolution into the ultra-microscopic region. *Phil. Mag.* **6**, 357–363.

Toledo-Crow, R., Yang, P.C., Chen, Y. & Vaez-Iravani, M. (1992) Near-field differential scanning optical microscope with atomic force regulation. *Appl. Phys. Lett.* **60**, 2957–2959.

Trautman, J.K., Betzig, E., Weiner, J.S., DiGiovanni, D.J., Harris, T.D., Hellman, F. & Gyorgy, E.M. (1992) Image contrast in near-field optics. *J. Appl. Phys.* **71**, 4659–4663.

Weisenhorn, A.L., Hansma, P.K., Albrecht, T.R. & Quate, C.F. (1989) Forces in atomic force microscopy in air and water. *Appl. Phys. Lett.* **54**, 2651–2653.